Modeling of the Thermodynamic Properties of Aqueous Ionic Liquid Solutions with an Equation of State for Square-Well Chain Fluid with Variable Range

ARTICLE *in* INDUSTRIAL & ENGINEERING CHEMISTRY RESEARCH · MAY 2011

Impact Factor: 2.59 · DOI: 10.1021/ie102156m

6 AUTHORS, INCLUDING:

Patrice Paricaud
ENSTA-ParisTech, Université Paris-Saclay
42 PUBLICATIONS **821** CITATIONS

I&EC research
Industrial & Engineering Chemistry Research

ARTICLE

pubs.acs.org/IECR

Modeling of the Thermodynamic Properties of Aqueous Ionic Liquid Solutions with an Equation of State for Square-Well Chain Fluid with Variable Range

Jinlong Li,[†,‡] Changchun He,[†] Changjun Peng,[†,*] Honglai Liu,[†] Ying Hu,[†] and Patrice Paricaud[‡]

[†]State Key Laboratory of Chemical Engineering and Department of Chemistry, East China University of Science and Technology, Shanghai 200237, China

[‡]Unité d'enseignement et de recherche de Chimie et Procédés (UCP), École Nationale Supérieure de Techniques Avancées (ENSTA), 75739 Paris, cedex 15, France

ABSTRACT: A new thermodynamic model based on an equation of state for square-well chain fluid with variable range (SWCF-VR) is proposed to describe the thermodynamic properties of aqueous solutions of ionic liquids. In this approach the electrostatic interactions are characterized via the mean spherical approximation and the ionic associations between the cations and anions of the ionic liquid are considered through the shield-sticky approach. The liquid densities, osmotic coefficients, and vapor pressures of aqueous solutions of nine ionic liquids (ILs) containing $[C_x\text{mim}][\text{Br}]$ ($x = 2, ..., 6$), $[C_4\text{mim}][BF_4]$ and $[C_x\text{mim}][MSO_4]$ ($x = 1, 3, 4$) have been modeled with the new model. Two ionic parameters for each anion and three for each cation of the ionic liquids were adjusted to experimental liquid densities and osmotic coefficients, and the corresponding average deviations are only 0.87% and 2.49%, respectively. Using the same ionic parameters, the vapor pressures of ionic liquid solutions are accurately predicted. The predicted equilibrium constants of the ionic association between the cations and anions of ILs in water were consistent with experimental observations.

1. INTRODUCTION

Ionic liquids (ILs) are melted salts of great industrial interest and are typically composed of large organic cations and small inorganic anions. ILs have many promising applications in a wide variety of fields in virtue of their special physicochemical properties such as low melting point (less than 373 K), wide liquid region, nonflammability, good thermal and chemical stability, high ionic conductivity, and negligible vapor pressure. For instance, they have been used as solvents in separations, catalysts in reactions, and lubricants in machinery, etc.[1,2] ILs have also been considered as good green replacements for conventional volatile organic solvents due to their unique environment-friendly characteristics.[3,4] In addition, the properties of ILs can be artificially tailored for a practical requirement by the right selections of the cations and anions. As a result, thousands of ILs can be designed and synthesized for specific applications in different fields. A growing attention has been paid to ILs in both academic and industrial studies in the past decade. Physical properties of pure ILs and their mixtures, such as pressure−volume−temperature (pVT), phase behavior, gas solubilities, viscosities, and caloric properties are required in practical applications. Some detailed reviews about experimental methods and data collections can be found in the literature.[5−7] Although a large amount of experimental data have been measured and reported, some appropriate theoretical models that are crucial for the design and optimization of chemical processes are required to correlate and predict thermodynamic properties. In recent years, many efforts have been devoted to the development of thermodynamic models of ILs.[8]

Some traditional empirical and semiempirical methods have been extensively used to correlate experimental thermodynamic data of ILs. The usual methods used to represent phase behavior of ILs are based on excess Gibbs free energy (g^E) models such as Wilson, NRTL, and UNIQUAC.[9,10] Simoni et al.[11,12] studied and compared the ability of several g^E models (NRTL, UNIQUAC, and electrolyte-NRTL (e-NRTL)) in predicting ternary liquid−liquid equilibria (LLE) from binary experimental results. Other classical methods like regular solution theory,[13] group contribution (GC) models,[14] and cubic equation of state (EOS)[15] were also applied to correlate and predict phase behavior of systems containing ILs. Although these models have been successfully used to describe the thermodynamic properties of ILs, they are not based on a detailed molecular description of the chemical species. In this context, several thermodynamic models based on statistical mechanics have been developed for IL systems. Kroon et al.[16] consider an ionic liquid (cation + anion) as a neutral associating chain with dipolar interactions. In this model, the molecular parameters like the size, the dispersion, and the association energies of IL were estimated through literature data of the corresponding cations and anions and the segment number was obtained by fitting experimental density data. The model can satisfactorily correlate the solubility of carbon dioxide (CO_2) in ILs over a wide pressure range. In their subsequent work,[17] they rescaled the molecular parameters of ILs with experimental pVT data and limited their EOS to estimate the phase equilibrium of ILs at low pressure again. Andreu and

Received: October 24, 2010
Accepted: April 28, 2011
Revised: April 26, 2011
Published: April 28, 2011

Vega[18] represent an ionic liquid as a Lennard-Jones flexible chain with an associating site and successfully modeled the CO_2 solubility in ILs by using the soft-SAFT EOS. ILs have also been modeled as neutral associating[19] or nonassociating[20] chain-like fluids interacting with square-well dispersion interactions, as well as a diblock component.[21,22] The readers are directed to a detailed review by Vega et al.[8]

Most of the empirical and theoretical EOS mentioned above can be well applied for describing phase behavior of ILs-containing systems in practice. However, from a theoretical point of view, it is required to explicitly take the electrostatic interactions into account for the prediction of bulk thermodynamic properties of ILs, and the ionic characteristic of ILs has been recognized and justified by both experimental observations and simulation studies.[23−25] Recently, some new experimental data of ionic liquid aqueous solutions further show that ILs behave more like a typical electrolyte solution.[26−32] Thus, the thermodynamic models for electrolyte solutions can be extended to systems containing ILs.

Charge−charge interactions between ions in aqueous solution have often been modeled by using the expressions[33,34] obtained from the solution of integral equations within the mean spherical approximation (MSA). One distinguishes two kinds of approaches: In the "primitive model" approach, the ions are represented as charged hard spheres immersed in a continuum media. The ions can then be of same diameter[35−38] or have different diameters.[33,34] In the "non primitive model" approach, an electrolyte solution is represented as a mixture of charged hard spheres representing the ions, and dipolar hard spheres representing the polar solvent. The statistical associating fluid theory (SAFT) has been combined to MSA charge−charge contributions to determine the thermodynamic properties of electrolyte systems. Liu et al.[39] developed a thermodynamic model for aqueous electrolyte solution based on the original SAFT EOS[40,41] and an MSA term, in which the ion−ion, ion−dipole, and dipole−dipole interactions are explicitely taken into account. An accurate description of the mean ionic activity coefficients (MIAC) and the densities were obtained for about 30 aqueous electrolyte solutions including 1:1-, 2:1-, and 1:2-type electrolytes. Jackson and co-workers[42,43] developed the SAFT-VRE model based on a combination of the SAFT-VR EOS with Coulombic ion−ion term (either MSA or Debye−Huckel). The SAFT-VRE model gives good predictions of the vapor pressures and liquid densities of aqueous solutions of 1:1 electrolytes. The SAFT-VRE model has also been used to predict the salting-out effect in water + alkane mixtures.[44] Radosz and co-workers assumed a salt as one single neutral molecule consisting of two segments (cation and anion) with different size and developed the SAFT1[45,46] and SAFT2[47−49] EOSs through a combination of SAFT[50] and the restrict primitive model of MSA. Their models can accurately describe the properties of single-salt, multisalt, and multivalent salt aqueous electrolyte solutions over wide temperature and pressure ranges. Liu et al.[51] applied the first order mean spherical approximation (FMSA) theory, based on a short-range Sutherland potential mapped with a two-Yukawa equation, to capture the different interactions between ions and solvents in electrolyte solution. They developed a statistical mechanics based EOS which successfully represented the properties of univalent and bivalent electrolyte solutions. By using the SAFT EOS and the low-density expansion of the nonprimitive MSA model, Liu et al.[52] developed a two-parameter EOS for electrolyte solutions, which accounts for solvent−solvent (dipole−dipole) and ion−solvent (charge-dipole) interactions. One key advantage of this model is that no empirical expression for the dielectric constant of the solvent is needed, in contrast to other models like SAFT2 and SAFT-VRE. In combination with the nonprimitive MSA model, the SAFT-VR[53] and PC-SAFT[54] EOSs have also been extended to the aqueous electrolyte solution by Zhao et al.[55] and Herzog et al.,[56] respectively. Sadowski and co-workers[57] combined the PC-SAFT EOS and the Debye−Hückel contribution for the coulomb interactions to develop an ePC-SAFT model for the electrolyte solution, and have applied it successfully to the strong[58] and weak[59] aqueous electrolyte solutions.

Paricaud et al.[60] gave a detailed overview of the development of the SAFT approach in representing the vapor−liquid equilibrium (vapor pressure and density) of aqueous solutions of strong electrolytes. A review of recent development and applications of SAFT in different fields containing electrolyte solutions was also given by Tan et al.[61] However, most of SAFT-based models for electrolyte solutions described above were applied to common ionic solutions, and the ionic molecule or the corresponding cation and anion was always assumed as a spherical particle.

Recently, Wang et al.[62] applied the MSA approach to ionic liquids to explicitly take the electrostatic interactions into account. In their model, the cation and anion of an ionic liquid are considered as separated species and modeled as univalent charged spheres. An accurate representation of the densities of pure ILs was obtained and the role of electrostatic interactions was checked and justified. The work of Wang et al.[62] represents a break through in the modeling of the properties of ionic liquids in a statistical mechanics framework, as the electrostatic interactions were explicitly considered for the first time in a macroscopic thermodynamic approach. However, the cations of ILs are often large organic species, and it seems more reasonable to assume as the cations and anions are chain-like groups with electrostatic interactions rather than charged spheres.

The preliminary work here aims at constructing a reasonable molecular structure for ILs and develops a statistical mechanics-based equation of state (EOS) to represent the thermodynamic properties of aqueous electrolyte solutions of ILs. Our approach is based on an equation of state that we previously developed for square-well chain fluids with variable range (SWCF-VR), using both perturbation theory[63] and integral equation[64] theories, which has successfully been applied to represent the phase behavior of prototype systems and the real pure fluids and mixtures.[20,65−68] In this model, the contribution due to hydrogen bonding between water molecules is calculated through the model of Liu et al.[69] and the long-range electrostatic interactions between ions is described by the MSA model.[34] The association between cations and anions is also considered in this model through the sticky-shield approach.[70,71] This paper is organized as follows. Section 2 gives a detailed description of the thermodynamic model. The determination of the molecular parameters for water and some ions of ILs is explained in section 3. In section 4, the results obtained for the predictions of the densities, osmotic coefficients, and vapor pressure for aqueous ILs solution are presented. A detailed discussion about the ionic association between the cations and anions of ILs in water are also provided. At last, conclusions are made in section 5.

2. THEORY

Let us consider a mixture containing chain molecules and charged ions. Ions are also considered as chain-like chemical

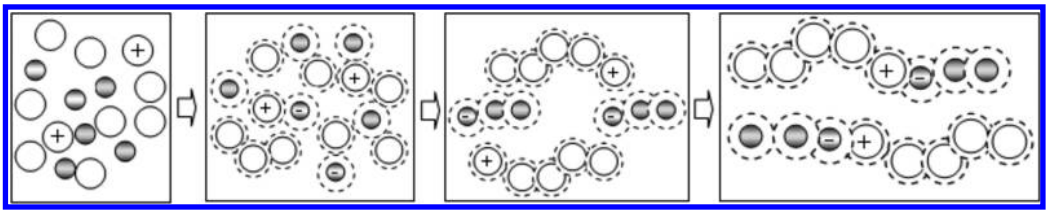

Figure 1. Formation of ionic pairs in a neutral solution without considering hydrogen association. The open circles are hard spherical segments of cations; the filled circles are spherical segments of anions; the dash circles denote the range of the square-well potentials.

species that are composed of a certain number of uncharged hard spherical segments and one charged hard spherical segment. The interactions between the charged and uncharged spherical segments of different molecules are composed of short-range repulsion and attraction (dispersion) and/or long-range (electrostatics) interactions as well as associations due to hydrogen bonding. Thus, an ionic liquid diluted in an aqueous solution is represented by two chemical species: a chain-like cation and a spherical anion. In this work, we take the association between anions and cations (ion paring) into account, that is, the ionic pairs and the corresponding free cations and anions can coexist in the solution. Note that we only consider the associations between ions of opposite charges while the association interactions between ions with the same negative or positive charge are neglected in this model. Figure1 gives an illustration of the formation of ionic pairs without considering hydrogen associations and interactions between solvent and solute. From left to right, the corresponding figures represent a system of hard spheres, hard spheres interacting via square-well (SW) potentials, ionic SW chains, and ionic pairs systems, respectively.

Let us now consider a mixture of S kinds of uncharged molecules and $2M$ kinds of chain-like ions. Each neutral molecule of type i (i = 1, ..., S) is composed of r_i spherical segments of diameter σ_i. Each ionic chain (cation or anion) contains $r_{\mathrm{cat},j} - 1$ or $r_{\mathrm{an},j} - 1$ (j = 1, ..., M) uncharged spherical segments and one spherical segment that can be either positively or negatively charged. Here, $r_{\mathrm{cat},j}$ and $r_{\mathrm{an},j}$ are the number of segments of a cationic and anionic chain, respectively. Furthermore, it is assumed that the diameter of the uncharged segments is equal to the diameter of the charged segment within the same ionic chain. Each cation and anion is characterized by its number of segments and the segment diameter. In this work, ILs are considered as 1:1 electrolytes and a solution of an IL will be composed of neutral chain molecules of solvent and ionic chains of IL solute. Hence, there will be $K = S + 2M$ different kinds of chain-like molecules or ions in the solution, and each ionic chain carries charge $z_i e$, where e is the elementary charge. Electroneutrality requires that

$$\sum_{i=1}^{K} \rho_{0,i} z_i = 0 \tag{1}$$

where $\rho_{0,i}$ is the number density of chemical species i. By using statistical mechanics and perturbation theory, one can express the residual Helmholtz free energy for this mixture as a sum of different contributions, that is,

$$\frac{\beta A^r}{V} = \frac{\beta \Delta A^{\mathrm{mono}}}{V} + \frac{\beta \Delta A^{\mathrm{chain}}}{V} + \frac{\beta \Delta A_{\mathrm{h}}^{\mathrm{assoc}}}{V} + \frac{\beta \Delta A^{\mathrm{msa}}}{V} + \frac{\beta \Delta A_{\mathrm{cat\text{-}an}}^{\mathrm{assoc}}}{V} \tag{2}$$

where V is volume of the system, $\beta = 1/(kT)$, k is the Boltzmann constant, and T is the temperature. ΔA^{mono} is the residual free energy of monomers; $\Delta A^{\mathrm{chain}}$ is the free energy contribution of the chain formation; ΔA^{msa} is the contribution due to the charge−charge electrostatic interactions. $\Delta A_{\mathrm{h}}^{\mathrm{assoc}}$ and $\Delta A_{\mathrm{cat\text{-}an}}^{\mathrm{assoc}}$ are the association contributions due to hydrogen bonding among solvent molecules and ion pairing, respectively. One particularity of the new model is that ions are here considered as chain-like chemical species, while ions are usually treated as charged spheres. Another key feature is the association contribution due to ion pairing.

2.1. Monomer Contribution. According to the Barker−Henderson perturbation theory[63] and our previous work,[65] the free energy of a monomer mixture can be expressed as the summation of a hard sphere repulsion (hs) term and square-well dispersion (sw-mono) terms, namely,

$$\frac{\beta \Delta A^{\mathrm{mono}}}{V} = \frac{\beta \Delta A^{\mathrm{hs}}}{V} + \frac{\beta \Delta A_1^{\mathrm{sw\text{-}mono}}}{V} + \frac{\beta \Delta A_2^{\mathrm{sw\text{-}mono}}}{V} \tag{3}$$

where the subscripts "1" and "2" denote the first- and second-order perturbation terms. The "hs" repulsive contribution is the residual free energy of a mixture of hard spheres with different sizes and is calculated by using the Mansoori−Carnahan−Starling−Leland EOS,[72]

$$\frac{\beta \Delta A^{\mathrm{hs}}}{V} = \left(\frac{\zeta_2^{\,3}}{\zeta_3^{\,2}} - \zeta_0\right) \ln \Delta + \frac{\pi \zeta_1 \zeta_2}{2\Delta} + \frac{\pi \zeta_2^{\,3}}{6 \zeta_3 \Delta^2} \tag{4}$$

where

$$\zeta_l = \sum_{i=1}^{K_s} \rho_{s,i} \sigma_i^l \ (l = 0, \ldots, 3), \quad \Delta = 1 - \frac{\pi}{6} \zeta_3 \tag{5}$$

here $\rho_{s,i}$ is the segment number density of specie i and K_s is the number of types of segments with or without charges.

The first and second-order perturbation terms due to SW dispersive interactions are given by

$$\frac{\beta \Delta A_1^{\mathrm{sw\text{-}mono}}}{V} = -\frac{2\pi}{3} \sum_{i=1}^{K_s} \sum_{j=1}^{K_s} \rho_{s,i} \rho_{s,j} (\lambda_{ij}^{\,3} - 1) \sigma_{ij}^{\,3} \left(\frac{\varepsilon_{ij}}{kT}\right) I_1(\eta, \lambda_{ij}) \tag{6}$$

and

$$\frac{\beta \Delta A_2^{\mathrm{sw\text{-}mono}}}{V} = -\frac{\pi}{3} K^{\mathrm{hs}} \sum_{i=1}^{K_s} \sum_{j=1}^{K_s} \rho_{s,i} \rho_{s,j} (\lambda_{ij}^{\,3} - 1) \sigma_{ij}^{\,3} \left(\frac{\varepsilon_{ij}}{kT}\right)^2 I_2(\eta, \lambda_{ij}) \tag{7}$$

where σ_{ij}, ε_{ij}, and λ_{ij} are the segment diameter, the depth, and the range of the SW potential between two segments of type i and j. The parameter of K^{hs} is the isothermal compressibility of a

mixture for hard spheres. The cross parameters are estimated from the generalized Lorentz−Berthelot mixing rule,[73] as

$$\sigma_{ij} = (\sigma_{ii} + \sigma_{jj})/2 \tag{8}$$

$$\varepsilon_{ij} = (1 - k_{ij})\sqrt{\varepsilon_{ii}\varepsilon_{jj}} \tag{9}$$

$$\lambda_{ij} = (\sigma_{ii}\lambda_{ii} + \sigma_{jj}\lambda_{jj})/(\sigma_{ii} + \sigma_{jj}) \tag{10}$$

here k_{ij} is an adjustable binary parameter. In eqs 6 and 7, the terms I_1 and I_2 derived from perturbation theory are functions of the packing fraction $\eta = \pi\zeta_3/6$ and of the reduced SW range λ_{ij}, and are given by

$$I_1(\eta, \lambda_{ij}) = \frac{\xi_1(\lambda_{ij})\eta + \xi_2(\lambda_{ij})}{2\eta(1-\eta)} - \frac{\xi_2(\lambda_{ij})}{2\eta(1-\eta)^2} + \xi_3(\lambda_{ij})\ln(1-\eta) + 1 \tag{11}$$

and

$$I_2(\eta, \lambda_{ij}) = \partial[\eta I_1(\eta, \lambda_{ij})]/\partial\eta \tag{12}$$

The parameters ξ_i (i = 1, 2, 3) used in eqs 11 and 12 are universal functions of λ_{ij} and are expressed as

$$\begin{pmatrix} \xi_1(\lambda_{ij}) \\ \xi_2(\lambda_{ij}) \\ \xi_3(\lambda_{ij}) \end{pmatrix} = \begin{pmatrix} -890.366 & 2510.86 & -2629.19 & 1212.91 & -208.167 \\ -957.906 & 2722.24 & -2872.35 & 1334.96 & -230.768 \\ 943.572 & -2808.87 & 3082.31 & -1481.70 & 263.780 \end{pmatrix} \begin{pmatrix} 1 \\ \lambda_{ij}^{0.5} \\ \lambda_{ij} \\ \lambda_{ij}^{1.5} \\ \lambda_{ij}^{2} \end{pmatrix} \tag{13}$$

The parameter K^{hs} in eq 7 is given by

$$K^{hs} = \zeta_0(1-\eta)^4 \Big/ \left(\zeta_0 + \left(6\frac{\zeta_1\zeta_2}{\zeta_3} - 2\zeta_0\right)\eta + \left(9\frac{\zeta_2^3}{\zeta_3^2} - 6\frac{\zeta_1\zeta_2}{\zeta_3} + \zeta_0\right)\eta^2 - 4\frac{\zeta_2^3}{\zeta_3^2}\eta^3 + \frac{\zeta_2^3}{\zeta_3^2}\eta^4\right) \tag{14}$$

2.2. Chain Formation Contribution. Following the suggestion of Hu et al.,[74] the contribution due to the formation of a chain with r SW monomer segments in a mixture can be estimated as

$$\frac{\beta\Delta A^{chain}}{V} = -\sum_{i=1}^{K_s} \rho_{s,i}\frac{r_i - 1}{r_i}\ln y^{sw(2e)}_{S_jS_{j+1}(ii)} - \sum_{i=1}^{K_s} \rho_{s,i}\frac{r_i - 2}{r_i}\ln y^{sw(2e)}_{S_jS_{j+2}(ii)} \tag{15}$$

here $y^{sw(2e)}_{S_jS_{j+1}(ii)}$ and $y^{sw(2e)}_{S_jS_{j+2}(ii)}$ are the effective two-particle cavity correlation functions (CCFs) of SW chains for the nearest-neighbor segment pair and the next-to-nearest-neighbor segment pair of component i, respectively. It is reasonable to assume that the CCFs can be expressed as the product of a hard sphere term and a perturbation term; that is,

$$y^{sw(2e)}_{S_jS_{j+1}} = y^{hs(2e)}_{S_jS_{j+1}} \times \Delta y^{sw(2e)}_{S_jS_{j+1}} \tag{16}$$

$$y^{sw(2e)}_{S_jS_{j+2}} = y^{hs(2e)}_{S_jS_{j+2}} \times \Delta y^{sw(2e)}_{S_jS_{j+2}} \tag{17}$$

where $y^{hs(2e)}_{S_jS_{j+1}}$ and $y^{hs(2e)}_{S_jS_{j+2}}$ are the effective two-particle CCFs of hard-sphere chains for the nearest-neighbor segment pair and the next-to-nearest-neighbor segment pair, respectively. $\Delta y^{sw(2e)}_{S_jS_{j+1}}$ and $\Delta y^{sw(2e)}_{S_jS_{j+2}}$ are defined as the nearest-neighbor and next-to-nearest-neighbor residual CCFs due to the effect of SW potential on chain formation of the hard sphere. Hu et al.[74] have proposed expressions for the nearest-neighbor and next-to-nearest-neighbor effective two-particle CCFs for hard spheres, on the basis of the computer simulation data. These expressions were given by

$$\ln y^{hs(2e)}_{S_jS_{j+1}(ii)} = \frac{\alpha_2\eta - \beta_2}{2(1-\eta)} + \frac{\beta_2}{2(1-\eta)^2} - \delta_2\ln(1-\eta) \tag{18}$$

$$\ln y^{hs(2e)}_{S_jS_{j+2}(ii)} = \frac{r-1}{r}\left[\frac{\alpha_3\eta - \beta_3}{2(1-\eta)} + \frac{\beta_3}{2(1-\eta)^2} - \delta_3\ln(1-\eta)\right] \tag{19}$$

where

$$\alpha_2 = 3 - a_2 + b_2 - 3c_2; \quad \beta_2 = 1 + c_2 - a_2 - b_2; \quad \delta_2 = c_2 + 1 \tag{20}$$

$$\alpha_3 = -a_3 + b_3 - 3c_3; \quad \beta_3 = c_3 - a_3 - b_3; \quad \delta_3 = c_3 \tag{21}$$

and

$$a_2 = 0.45696; \quad b_2 = 2.10386; \quad c_2 = 1.75503 \tag{22}$$

$$a_3 = -0.74745; \quad b_3 = 3.49695; \quad c_3 = 4.83207 \tag{23}$$

The SW contribution on chain formation for the CCF between nearest-neighbor segments is calculated by

$$\ln \Delta y^{sw(2e)}_{S_jS_{j+1}(ii)} = \ln\left(g^{sw(2e)}_{S_jS_{j+1}(ii)} \Big/ g^{hs(2e)}_{S_jS_{j+1}(ii)}\right) \tag{24}$$

where $g^{sw(2e)}_{S_jS_{j+1}}$ is the radial distribution function between SW segments. The expression for $g^{sw(2e)}_{S_jS_{j+1}}$ can be obtained from perturbation theory and the Clausius virial theorem as

$$g^{sw(2e)}_{S_jS_{j+1}(ii)} = g^{hs}_{S_jS_{j+1}(ii)}(\sigma_{ii}) + \frac{\varepsilon_{ii}}{kT}\left[I_1(\eta, \lambda_{ii}) + (\lambda_{ii}^3 - 1) \times \left(\frac{\lambda_{ii}}{3}\frac{\partial I_1(\eta, \lambda_{ii})}{\partial\lambda_{ii}} - \eta\frac{\partial I_1(\eta, \lambda_{ii})}{\partial\eta}\right)\right] \tag{25}$$

The radial distribution function $g^{hs}_{S_jS_{j+1}}$ in a hard sphere mixture is given by

$$g^{hs}_{S_jS_{j+1}(ii)}(\sigma_{ii}) = \frac{1}{1-\eta} + 3\frac{D_{ii}\eta}{(1-\eta)^2} + 2\frac{(D_{ii}\eta)^2}{(1-\eta)^3} \tag{26}$$

where D_{ii} is defined as

$$D_{ii} = \frac{\sigma_{ii}}{2}\frac{\zeta_2}{\zeta_3} \tag{27}$$

dx.doi.org/10.1021/ie102156m |Ind. Eng. Chem. Res. 2011, 50, 7027–7040

In eq 17, the next-to-nearest-neighbor residual CCF of component i is given by[65]

$$\ln \Delta y^{\mathrm{sw}(2\varepsilon)}_{\mathrm{S}_j\mathrm{S}_{j+2}(ii)} = \frac{r_{ii}-1}{r_{ii}}\frac{\varepsilon_{ii}}{kT}\left(\frac{\xi_a(\lambda_{ii})\eta+\xi_b(\lambda_{ii})}{2(1-\eta)}-\frac{\xi_b(\lambda_{ii})}{2(1-\eta)^2}+\xi_c(\lambda_{ii})\ln(1-\eta)\right) \quad (28)$$

with

$$\begin{cases}\xi_a(\lambda_{ii}) = (\xi_1(\lambda_{ii})+\xi_2(\lambda_{ii})+6)/4\\ \xi_b(\lambda_{ii}) = (\xi_1(\lambda_{ii})-\xi_2(\lambda_{ii})+\xi_3(\lambda_{ii})+5)/7\\ \xi_c(\lambda_{ii}) = (2\xi_1(\lambda_{ii})-\xi_3(\lambda_{ii})+2)/3\end{cases} \quad (29)$$

2.3. Association Contribution from Hydrogen Bonding. To represent hydrogen bonding interactions, Liu et al.[69] proposed a model based on the shielded sticky-shell approach, in which an associating fluid is supposed to have only one associating site. The expression of the association free energy contribution is similar to that obtained from the TPT1 theory[75−78] and is given by

$$\frac{\beta\Delta A^{\mathrm{assoc}}}{V} = \sum_{i=1}^{K}\rho_{0,i}\left[\ln X_i+\frac{1}{2}(1-X_i)\right] \quad (30)$$

where $\rho_{0,i}$ is the number density of molecule i; X_i is the mole fraction of not-bonded molecule i and can be solved by an iterative method from the following equation:

$$X_i = (1+\sum_j \rho_{0,j}X_j\Delta_{ij})^{-1} \quad (31)$$

and

$$\rho_{0,j}\Delta_{ij} = \frac{\pi}{3}{\sigma_{ij}}^3\kappa_{ij}{\iota_{ij}}^{-1}\rho_{0,j}y^{\mathrm{ref}} \quad (32)$$

here κ_{ij} is the fraction of the segment surface participating in the association. The parameter ${\iota_{i,j}}^{-1} = (\exp(\beta\delta\varepsilon^{\mathrm{assoc}}_{\mathrm{H},ij}) - 1$ is a sticky parameter and $\delta\varepsilon^{\mathrm{assoc}}_{\mathrm{H},ij}$ is the association energy parameter. In eq 32, y^{ref} is an effective CCF between associating segments S_i and S_j and can be written as[69]

$$\ln y^{\mathrm{ref}} = \frac{1}{\zeta_0}\left[\frac{\alpha_2\zeta_1\zeta_2\eta/\zeta_3-\beta_2{\zeta_2}^3/{\zeta_3}^2}{2(1-\eta)}+\frac{\beta_2{\zeta_2}^3/{\zeta_3}^2}{2(1-\eta)^2}-\delta_2\frac{{\zeta_2}^3}{{\zeta_3}^2}\ln(1-\eta)\right] \quad (33)$$

where the parameters of α_2, β_2, and δ_2 are the same as those for hard spheres.

2.4. Charge−Charge MSA Contribution. The free energy due to the long-range Coulombic interactions between ions is the expression obtained by using Blum from the solution of Ornstein−Zernike integral equation, which is given by[34]

$$\frac{\beta A^{\mathrm{msa}}}{V} = -\frac{\beta e^2}{4\pi D}\sum_{\mathrm{ions}}\frac{\rho_{\mathrm{s},i}z_i}{1+\sigma_i\Gamma}\left(z_i\Gamma+\frac{\pi\sigma_i P_n}{2\Delta}\right)+\frac{\Gamma^3}{3\pi} \quad (34)$$

where $D = \varepsilon_0 D_r$, ε_0 is the permittivity of vacuum and D_r the dielectric constant the solvent. We assume that D_r is the dielectric constant of saturated liquid water, which can be estimated from the following correlation:[45]

$$D_r = 281.67 - 1.0912T + 1.6644\times10^{-3}T^2 - 9.7592\times10^{-7}T^3 \quad (35)$$

The sum in eq 34 is over the number of types of charged segments. Note that the density required in eq 34 is one containing the contributions of both solute and solvent particles although the primitive MSA approach is employed in current work.

The expressions for Γ and P_n are given by

$$\Gamma = \frac{e}{2}\sqrt{\frac{\beta}{D}}\left(\sum_{\mathrm{ions}}\rho_{\mathrm{s},i}\left(\frac{z_i-\pi\sigma_i{}^2P_n/2\Delta}{1+\sigma_i\Gamma}\right)^2\right)^{1/2} \quad (36)$$

and

$$P_n = \sum_{\mathrm{ions}}\frac{\rho_{\mathrm{s},i}\sigma_i z_i}{1+\sigma_i\Gamma}\Bigg/\left(1+\frac{\pi}{2\Delta}\sum_{\mathrm{ions}}\frac{\rho_{\mathrm{s},i}\sigma_i^3}{1+\sigma_i\Gamma}\right) \quad (37)$$

The two equations above can be solved through a simple iterative method.

2.5. Contribution of Ionic Association. The associating interaction between ions i and j can be described by adopting the shield-sticky approach.[70,71] One defines the Mayer function f_{ij} for ionic pairs as

$$f_{ij} = \begin{cases}-1+{\tau_{ij}}^{-1}\sigma_{ij}\delta(r-\sigma_{ij})/12 & r\le\sigma_{ij}\\ \exp(-\beta\Delta E_{ij})-1 & r>\sigma_{ij}\end{cases} \quad (38)$$

where ${\tau_{ij}}^{-1}$ is a parameter measuring stickiness, and ΔE_{ij} is the interaction energy between ions i and j at the distance beyond the collision diameter σ_{ij}. The total correlation function $h_{ij}(r)$ between particle i and j is related to the radial distribution function through $h_{ij}(r) = g_{ij}(r) - 1$ and is written as

$$h_{ij}(r) = -1+\Lambda_{ij}\sigma_{ij}\delta(r-\sigma_{ij})/12 \quad (39)$$

where Λ_{ij} is a distribution parameter that depends on the sticky parameter ${\tau_{ij}}^{-1}$. Suppose that $\alpha_{ij} = \rho_{ij}/\rho_{\mathrm{s},i}$ is the degree of association of ion i and $\alpha_{ji} = \rho_{ji}/\rho_{\mathrm{s},j}$ the degree of association of ion j. It is obvious that $\rho_{\mathrm{s},i}\alpha_{ij} = \rho_{\mathrm{s},j}\alpha_{ji}$. The degree of association between ions i and j can also be defined as

$$\alpha_{ij} = \rho_{\mathrm{s},i}\rho_{\mathrm{s},j}\int_{\sigma_{ij}^-}^{\sigma_{ij}^+} g_{ij}(r)\,\mathrm{d}r/\rho_{\mathrm{s},i} = \rho_{\mathrm{s},j}\int_{\sigma_{ij}^-}^{\sigma_{ij}^+} g_{ij}(r)\,\mathrm{d}r \quad (40)$$

By combining eqs 39 and 40, one can obtain

$$\alpha_{ij} = \frac{\pi}{3}\rho_{\mathrm{s},j}\omega_{ij}\Lambda_{ij}{\sigma_{ij}}^3 \quad (41)$$

where ω_{ij} is the fraction of the ionic surface participating in the ionic association, namely, a bonding volume parameter. The cavity correlation function between ions i and j at contact can be expressed from its definition $y_{ij}(r) = \exp(\beta\Lambda_{ij}(r))\,g_{ij}(r)$

$$y_{ij}(\sigma_{ij}) = \frac{1}{{\tau_{ij}}^{-1}\sigma_{ij}\delta(r-\sigma_{ij})/12}\Lambda_{ij}\sigma_{ij}\delta(r-\sigma_{ij})/12 = \tau_{ij}\Lambda_{ij} \quad (42)$$

dx.doi.org/10.1021/ie102156m |Ind. Eng. Chem. Res. 2011, 50, 7027–7040

On the basis of standard statistical thermodynamic relations, one can write

$$\delta(\beta A/V)/\delta f_{ij} = -\rho_{s,i}\rho_{s,j}y_{ij}(r) \quad (43)$$

The differential of the Mayer function is given by

$$\delta f_{ij} = \sigma_{ij}\delta(r-\sigma_{ij})\delta\tau_{ij}^{-1}/12 \qquad r \le \sigma_{ij} \quad (44)$$

Here $\delta(r-\sigma_{ij})$ is a Dirac delta function. Substituting eq 44 into eq 43 and then integrating it with respect to r and τ_{ij}^{-1}, one can express the association contribution as

$$\frac{\beta A^{\text{assoc}}_{\text{cat}-\text{an}}}{V} = \frac{\pi}{3}\rho_{s,i}\rho_{s,j}\omega_{ij}\alpha_{ij}^{3}\int_0^{\tau_{ij}^{-1}} y_{ij}(\sigma_{ij})\, d\tau_{ij}^{-1} \quad (45)$$

where ω_{ij} is a bonding volume parameter that is set to 1 due to no orientation of association between ions. One can express $d\tau_{ij}^{-1}$ from eqs 41 and 42 as

$$d\tau_{ij}^{-1} = \frac{3}{\pi\omega_{ij}\rho_{s,j}\sigma_{ij}^{3}}\left(\frac{1}{y_{ij}(\sigma_{ij})} - \frac{\alpha_{ij}}{y_{ij}^{2}(\sigma_{ij})}\left(\frac{\partial y_{ij}(\sigma_{ij})}{\partial\alpha_{ij}}\right)\right) d\alpha_{ij} \quad (46)$$

By combining eqs 45 and 46, we can write the free energy due to association between cation and anion as

$$\begin{aligned}\frac{\beta A^{\text{assoc}}_{\text{cat}-\text{an}}}{V} &= -\rho_{s,i}\left[\alpha_{ij} - \int_0^{\alpha_{ij}} \alpha_{ij}\, d\ln y_{ij}(\sigma_{ij})\right] \\ &= -\rho_{s,j}\left[\alpha_{ji} - \int_0^{\alpha_{ji}} \alpha_{ji}\, d\ln y_{ij}(\sigma_{ij})\right]\end{aligned} \quad (47)$$

Because of the difficulty of obtaining the CCF of real fluid from a theoretical point of view, we made the following assumption[74]

$$y_{ij}(\sigma_{ij}) = (1-\alpha_{ij})(1-\alpha_{ji})y_{ij}^{\text{ref}}(\sigma_{ij}) \quad (48)$$

In eq 48, the first two terms represent the contributions from association and the third one is the CCF of the reference nonassociating fluid. After substituting eq 48 into eq 47 and integrating, one obtains

$$\begin{aligned}\frac{\beta A^{\text{assoc}}_{\text{cat}-\text{an}}}{V} &= \rho_{s,i}\ln(1-\alpha_{ij}) + \rho_{s,j}\ln(1-\alpha_{ji}) \\ &\quad + \frac{1}{2}(\rho_{s,i}\alpha_{ij} + \rho_{s,j}\alpha_{ji})\end{aligned} \quad (49)$$

One must determine the degree of association between ions i and j to compute the free energy due to the association between cations and anions. By combining eqs 41, 42, and 48, τ_{ij}^{-1} can be expressed as

$$\tau_{ij}^{-1} = \frac{3\alpha_{ij}}{\pi\omega_{ij}\rho_{s,j}\sigma_{ij}^{3}(1-\alpha_{ij})(1-\alpha_{ji})y_{ij}^{\text{ref}}(\sigma_{ij})} \quad (50)$$

Let us define χ_{ij} as

$$\chi_{ij} = \frac{\pi}{3}\omega_{ij}\tau_{ij}^{-1}\sigma_{ij}^{3}y_{ij}^{\text{ref}}(\sigma_{ij}) \quad (51)$$

τ_{ij}^{-1} can be considered as an adjustable parameter and written as $\tau_{ij}^{-1} = \exp(\beta\delta\varepsilon_{ij}^{\text{assoc}})$.

Equations 50 and 51 lead to

$$\rho_{s,j} - (\rho_{s,i} + \rho_{s,j} + 1/\chi_{ij})\alpha_{ij} + \rho_{s,i}\alpha_{ij}^{2} = 0 \quad (52)$$

Equation 52 can be analytically solved in terms of α_{ij}, as

$$\begin{aligned}\alpha_{ij} = {} & ([\chi_{ij}(\rho_{s,i}+\rho_{s,j})+1] \\ & - \sqrt{[\chi_{ij}(\rho_{s,i}+\rho_{s,j})+1]^{2} - 4\chi_{ij}^{2}\rho_{s,i}\rho_{s,j}})/(2\rho_{s,i}\chi_{ij})\end{aligned} \quad (53)$$

Then, one can obtain α_{ji} based on the relationship of $\rho_{s,i}\alpha_{ij} = \rho_{s,j}\alpha_{ji}$.

The CCF of ions at contact can be obtained from the radial distribution function and the direct correlation function using the HNC approximation. The expression of the radial distribution function derived from the MSA[33,34,79] is given by

$$g_{ij}^{\text{ref}}(\sigma_{ij}) = \frac{1}{\Delta} - \frac{a_i a_j\Gamma^{2}}{\pi\sigma_{ij}\alpha_0^{2}} + \frac{\pi\sigma_i\sigma_j\zeta_2}{4\sigma_{ij}\Delta^{2}} \quad (54)$$

where $\alpha_0^{2} = \beta e^{2}/D$, and a_i is given by

$$a_i = \frac{\alpha_0^{2}}{2\Gamma(1+\sigma_i\Gamma)}\left(z_i - \frac{\pi\sigma_i^{2}P_n}{2\Delta}\right) \quad (55)$$

The corresponding direct correlation function is given by

$$c_{ij}^{\text{ref}}(\sigma_{ij}) = -\frac{\alpha_0^{2}z_iz_j}{4\pi\sigma_{ij}} \quad (56)$$

By applying the HNC, the CCF can be determined from

$$y_{ij}^{\text{ref}}(\sigma_{ij}) = \exp[g_{ij}^{\text{ref}}(\sigma_{ij}) - 1 - c_{ij}^{\text{ref}}(\sigma_{ij})] \quad (57)$$

Combining eqs 54, 56, and 57, one can express the cavity function as

$$\ln y_{ij}^{\text{ref}}(\sigma_{ij}) = \frac{1}{\Delta} + \frac{\alpha_0^{2}z_iz_j}{4\pi\sigma_{ij}} + \frac{\pi\sigma_i\sigma_j\zeta_2}{4\sigma_{ij}\Delta^{2}} - \frac{a_ia_j\Gamma^{2}}{\pi\sigma_{ij}\alpha_0^{2}} - 1 \quad (58)$$

Once the free energy expression for ionic liquid aqueous solution is developed, all the other thermodynamic properties can be derived through standard relationships. For example, the compressibility factor can be obtained by differentiating the free energy with respect to the density as

$$Z = 1 + \rho\left[\frac{\partial}{\partial\rho}\left(\rho\frac{\beta A^{r}}{V}\right)\right] \quad (59)$$

and the chemical potential of species k can be derived from the following differentiation

$$\beta\mu_k^{r} = \left[\frac{\partial}{\partial\rho_k}\left(\frac{\beta A^{r}}{V}\right)\right]_{T,\rho_{i(i\neq k)}} \quad (60)$$

3. MODEL PARAMETER ESTIMATION

Before calculating the properties of aqueous electrolyte solution of ILs, one first needs to describe the properties of pure water as accurately as possible. Here, water is modeled as a spherical molecule (i.e., $r = 1$) with one association site using the association model of Liu et al.[69] derived from the shielded sticky-shell method. The parameters for the water model are reported in Table 1. The relative average deviations of the vapor pressures and saturated liquid densities are 0.09% and 0.30%, respectively, for the temperature range from 278.15 to 393.15 K. In Figure 2, a comparison between theoretical and experimental vapor

Table 1. Model Parameters for Pure Water

parameter	abbreviation	value	unit
segment number	r	1.0	-
segment diameter	σ_0	2.9353	Å
dispersion energy	ε/k	596.29	K
reduced well width	λ	1.5005	-
association energy	ε_H^{asso}/k	3156.6	K
association volume	$\Delta\omega$	3.3985×10^{-4}	-

pressure and liquid density[80] has been illustrated, in which the correlated results from PC-SAFT[57] are also given. One can see that a good agreement between the models and the experimental data is obtained except for the liquid densities at temperatures around 277.15 K, which cannot be well described by any-state-of-the-art model[57] since it has a density maximum at about this temperature.

Several assumptions have to be made to calculate the properties of aqueous IL solutions such as densities, vapor pressures, and osmotic coefficients. First, the vapor phase above the solution is assumed to consist of pure water only due to the nonvolatile property of ILs. Second, the IL solution investigated in this work is considered as a 1:1 weak electrolyte solution. In other words, the IL solutes can partially dissociate into their respective cations and anions only. Thus, the cations, anions, and the neutral IL molecules coexist in the aqueous solution. Third, the dispersion interactions between ions of the same charge are neglected, so only the water−water, water−ion, and cation−anion interactions are considered. The parameter k_{ij} in eq 9 is equal to 0 except for $k_{22} = k_{33} = 1$, where the superscripts "22" and "33" represent the "cation−cation" and "anion−anion" interactions, respectively. The last assumption is that hydrogen bonding interactions are considered only among water molecules, and the effect of the polar character of water on the ion−ion interactions is considered via the dielectric constant of water.

In our present work, each real cation is considered as a chain-like species, while each anion is modeled as a spherical particle. There are four model parameters (r, σ, ε/k, and λ) characterizing each ion and one ionic association energy parameter ($\delta\varepsilon_{cat\text{-}an}^{asso}/k$) for each cation−anion pair interaction. For cations, the segment number parameter is determined by the following expression: $r_{cat} = 1.0 + 0.2N_C$, where N_C is the number of carbon atoms of the cation except those contained in the imidazolium ring. In this linear expression, the number "1.0" denotes the contribution from imidazolium ring.

As mentioned earlier, anions are considered as spherical species, thus, their segment number is equal to 1. In addition, the reduced well-width parameter for all anions is fixed to 1.5 while it is considered as an adjustable model parameter for all cations. Therefore, there are two molecular parameters for each anion (σ_i and ε_i/k) and three model parameters (σ_i, ε_i/k, and λ_i) for each cation. For the formation of ionic pairs, one ionic association parameter $\delta\varepsilon_{cat\text{-}an}^{asso}/k$ is required to describe the properties of ionic association in aqueous IL solution.

The experimental data that are used to adjust these parameters are the liquid densities and the osmotic coefficients of the aqueous IL solutions. Few mean ionic activity coefficient (MIAC) data are available in literature for these systems, although MIAC are very sensitive to the ionic parameters.[81] The osmotic coefficient in an aqueous IL solution is determined

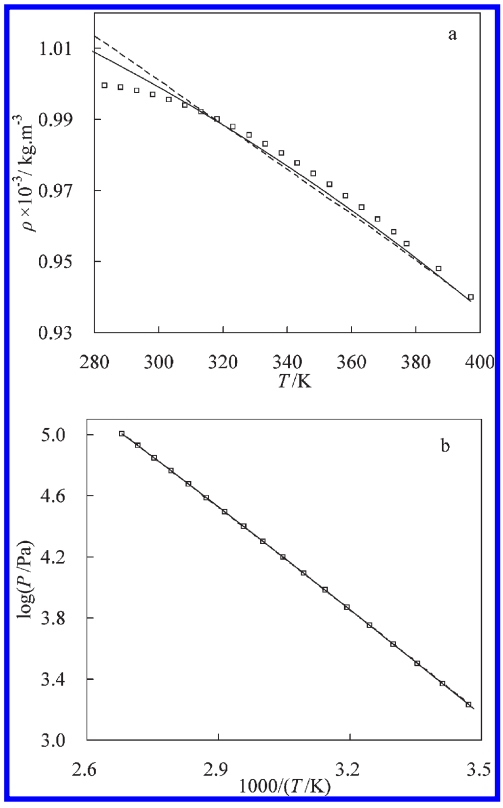

Figure 2. Saturated liquid densities (a) and vapor pressures (b) of pure water. Comparison between the theoretical calculations (lines) and the experimental data[80] (symbols): solid lines, this work; dash lines, PC-SAFT[57].

from[52]

$$\phi = \ln a_w / \ln x_w \tag{61}$$

where $a_w = \gamma_w x_w$ and x_w are the activity and the mole fraction of water. The activity coefficient of water in a solution, γ_w, at temperature T and pressure P is calculated in the mole fraction scale from

$$\ln \gamma_w = \ln \frac{\rho}{\rho_{w0}} + \frac{\mu_w^r - \mu_{w0}^r}{kT} \tag{62}$$

where the subscript "w0" means that the solvent (water) is in its reference pure state at T and P.

Following the work of Cameretti and Sadowski[57] and Held et al.,[58] we have determined ionic parameters rather than salt parameters, by fitting the properties of nine different aqueous IL solutions, simultaneously. Thus, the ionic parameters of an ion are applicable to all considered ILs containing this ion. For example, the parameters (r, σ, ε/k, and λ) for the anion of Br^- have the same values for the ILs [$C_x$mim][Br] (x = 2, ..., 6). The optimized ionic parameters are reported in Tables 2 and 3. From Table 2, one can see that the dispersion energies of the cations $[C_x\text{mim}]^-$ decrease from the smallest to the largest ion. The dispersion energies for the anions follow a similar trend. This result is consistent with the fact that ions with smaller diameter have larger charge density and interact more strongly with water molecules. A similar trend is observed for common electrolyte solutions.[45,57,58] Moreover, one can observe from Table 2 that the segment diameter of the cations slightly decreases with

increasing molecular weight and the ionic size ($r_i\sigma_i$) of the cations generally increase with respect to their increasing mass, but there is no a clear trend for the reduced well-width of the cations. For the anions, it can be seen that the segment diameter decreases with the increasing molecular weight, as shown in Table 2. From a physical point of view, it seems to be difficult to understand the strange trend, which has also been observed in common aqueous electrolyte solutions. For instance, there were trends for the segment diameter of anions [NO_3^- > SO_4^{2-}] in the work of Tan et al.[47] and [SCN^- > $ClO3^-$ > $BrO3^-$] in the work of Held et al.[58] observed, respectively. On one hand, this might be explained by the deficiency of the theoretical models for water and the ions,[42,57] and by a compensation effect between the parameters of the model. For instance, polarizability effects between ions and water have a great influence on thermodynamic properties, but these effects are not explicitly taken into account in the above approaches. On the other hand, the reason may be attributed to the fact that the anions Br^-, BF_4^-, and MSO_4^- contained in the present work are not homologous particles and have completely different apparent properties in aqueous solutions, namely they have no comparable relationship in essence between them.

One can further observe that ionic association energy parameter increases as the length of the alkyl chain of the cation increases for the series [$C_x$mim][Br] (x = 2, ..., 6). This trend is generally consistent with experimental observation.[25] For the ionic association ability of anions, it can also be seen from Table 3 that the strength of the association between cation $[C_4mim]^+$ and different anions follows the trend of $[Br]^-$ > $[BF_4]^-$ > $[MSO_4]^-$. This trend is the same as the one determined in gaseous state by using electrospray ionization mass spectrometry,[82] but opposite to that observed from the conductivity measurement method.[25] A more detailed discussion about the ionic association between the cations and anions of IL in aqueous systems will be given in section 4.4. Note that Table 3 is not complete as experimental data are not available for all possible ILs formed from the combinations of the anions and cations.

Here, it needs to stress that these parameters listed in Tables 2 and 3 are not valid for other IL related systems other than aqueous solutions. If one wants to predict some properties of pure ILs or nonaqueous IL mixtures in virtue of these parameters, other parameters (e.g., solvation parameters of ions or binary adjustable parameters) must be introduced to eliminate the effects of water on model parameters since the ions have different apparent size and energy in between aqueous and nonaqueous mixtures.

Table 2. Parameters for Cations and Anions of ILs

name	abbreviation	r	σ (Å)	ε/k (K)	λ
1,3-dimethylimidazolium	$[C_1mim]^+$	1.4	5.0158	520.17	1.5042
1-ethyl-3-methylimidazolium	$[C_2mim]^+$	1.6	4.9242	507.76	1.5319
1-propyl-3-methylimidazolium	$[C_3mim]^+$	1.8	4.8514	437.62	1.5463
1-butyl-3-methylimidazolium	$[C_4mim]^+$	2.0	4.4250	387.25	1.5286
1-pentyl-3-methylimidazolium	$[C_5mim]^+$	2.2	4.0026	309.51	1.5398
1-hexyl-3-methylimidazolium	$[C_6mim]^+$	2.4	3.8407	269.05	1.5280
bromine	$[Br]^-$	1.0	3.7563	471.91	1.5
tetrafluoroborate	$[BF_4]^-$	1.0	3.4215	178.98	1.5
methylsulfate	$[MSO_4]^-$	1.0	1.7529	44.689	1.5

Table 3. Association Energy Parameter $\delta\varepsilon^{assoc}_{cat-an}/k$ (K) between Cations and Anions for Different ILs[a]

	$[C_1mim]^+$	$[C_2mim]^+$	$[C_3mim]^+$	$[C_4mim]^+$	$[C_5mim]^+$	$[C_6mim]^+$
$[Br]^-$	-	23.551	68.975	76.163	84.778	495.31
$[BF_4]^-$	-	-	-	27.211	-	-
$[MSO_4]^-$	10.705	-	686.25	12.732	-	-

[a] The symbol "-" means that no data were available to adjust the parameter $\delta\varepsilon^{assoc}_{cat-an}/k$ (K).

4. MODELING RESULTS

The vapor−liquid equilibria, liquid densities, and the osmotic coefficients of ionic liquid + water systems have been calculated by using the new model and the parameters listed in Tables 2 and 3. The VLE data are not used for the model parameters estimation. The temperature range, the maximum molality (m_{max}), the absolute average deviation (AAD), the absolute maximum deviation (AMD), and the number of experimental data points (NP) are reported in Table 4 for nine types of aqueous IL solutions. The liquid densities and osmotic coefficients of aqueous solution of ILs are reasonably modeled by the new model with overall AAD values of 0.87% and 2.49%, respectively.

Table 4. Number of Data Points (NP), Average and Maximum Relative Deviations for the Osmotic Coefficients, and Densities of Aqueous Solutions of ILs

			$\Delta\phi$%			$\Delta\rho$%			
System	T/K	m_{max}/mol·kg^{-1}	NP	AAD[a]	AMD[a]	NP	AAD[a]	AMD[a]	ref.
[C_2mim][Br]	293−313	0.4435	12	1.13	2.23	50	0.72	1.61	26
[C_3mim][Br]	288−328	2.7049	80	1.51	8.12	85	0.25	0.77	27,28
[C_4mim][Br]	298−318	7.7923	12	1.03	3.56	45	0.36	0.97	29,30
[C_5mim][Br]	298−328	2.0049	80	1.61	8.10	-	-	-	27
[C_6mim][Br]	288−328	2.3976	76	2.66	11.9	70	0.88	2.05	27,28
[C_4mim][BF_4]	318	1.0232	12	3.21	6.71	-	-	-	29
[C_1mim][MSO_4]	313−333	3.2928	30	4.23	7.46	-	-	-	31
[C_3mim][MSO_4]	298−328	1.5690	39	3.25	8.85	56	2.15	7.01	32
[C_4mim][MSO_4]	313−333	4.0910	30	3.79	7.99	-	-	-	31
Overall average deviation			371	2.49	7.21	306	0.87	2.48	

[a] AAD% = $(100/NP)\sum_{i=1}^{NP}|(\theta_i^{expt} - \theta_i^{calc})/\theta_i^{expt}|$%, AMD% = 100 max($|(\theta_i^{expt} - \theta_i^{calc})/\theta_i^{expt}|$)% i = 1, ..., NP. The symbol, θ, denotes the osmotic coefficient or liquid density.

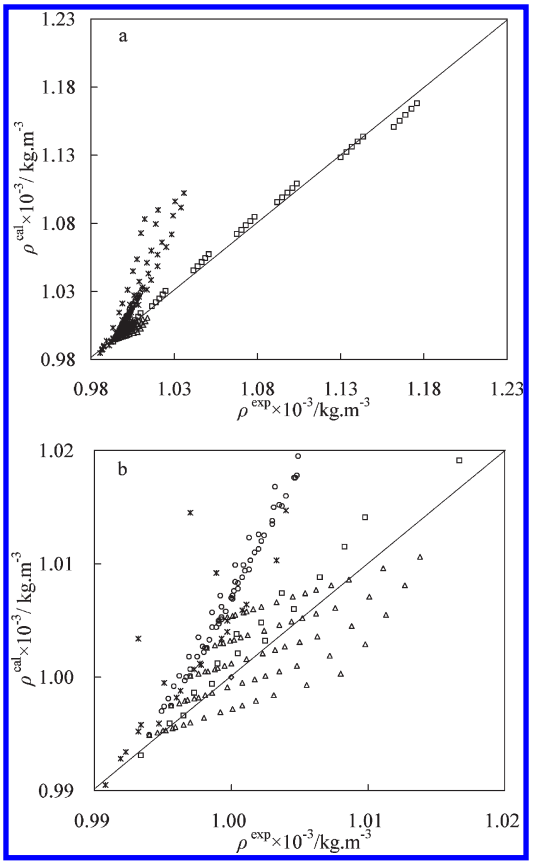

Figure 3. Liquid densities of aqueous IL solutions. Comparison between the new model and the experimental data.[26−30,32] Panel b is an enlargement of panel a within a smaller density range: (◊) [C_2mim][Br]; (Δ) [C_3mim][Br]; (□) [C_4mim][Br]; (○) [C_6mim][Br]; (∗) [C_3mim][MSO_4].

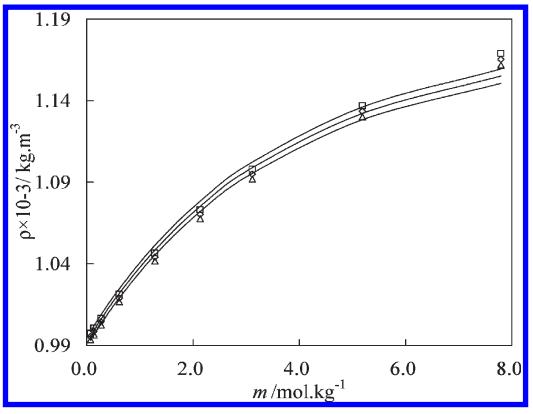

Figure 4. Liquid densities for aqueous solutions of [C_4mim][Br] at different temperatures. Comparison between the new model (lines) and the experimental data[29,30] (symbols): (□) 308; (◊) 313; (Δ) 318 K.

4.1. Liquid Density. A comparison between the calculated and experimental liquid densities of IL aqueous solutions has been given in Figure 3. Figure 3b is an enlargement of Figure 3a within a smaller density range. The calculated densities are in an excellent agreement with the experiment data except [C_3mim][MSO_4], which has a comparably larger deviation (2.15%) compared to the rest. As an example, the liquid densities

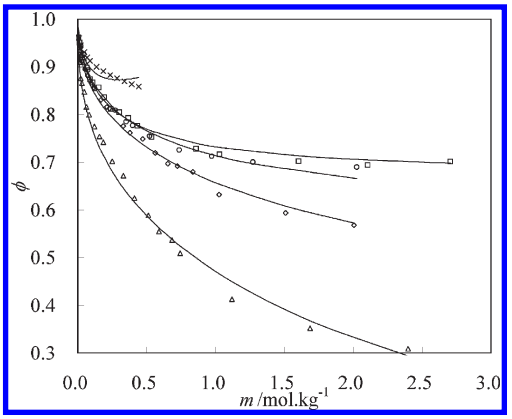

Figure 5. Osmotic coefficients of [$C_x$mim][Br] (x = 3,4,5,6) at 318 K and [C_2mim][Br] at 298 K. Comparison between the new model (lines) and the experimental data[26−30] (symbols): (×) C_2; (□) C_3; (○) C_4; (◊) C_5; (Δ) C_6.

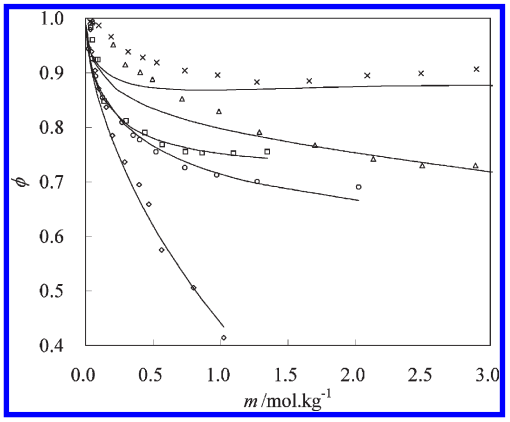

Figure 6. Osmotic coefficients of different IL solutions. Comparison between the new model (lines) and the experimental data[29−32] (symbols): (×) [C_1mim][MSO_4] at 313 K; (□) [C_3mim][MSO_4] at 318 K; (Δ) [C_4mim][MSO_4] at 313 K; (○) [C_4mim][Br] at 318 K; (◊) [C_4mim][BF_4] at 318 K.

of aqueous solutions of [C_4mim][Br] as a function of molality at different temperatures are depicted in Figure 4, and the experimental data are accurately described by the new model in the region of lower concentration of ILs, while the deviation slightly increases in the region of higher molality.

4.2. Osmotic Coefficient. The osmotic coefficient of a given solution is a property that can be used to characterize the deviation of the activity of the solvent from the ideal behavior. As a typical example, the osmotic coefficients of aqueous solutions of [$C_x$mim][Br] (x = 2,3,...,6) as a function of the IL molality are shown in Figure 5. It can be seen that the osmotic coefficients generally decrease with increasing alkyl chain length of cation, at a given IL molality, corresponding to a strengthening of the effects of the IL solute on the solvent activity. This behavior cannot be understood from a change of surface charge density, but may be explained by the fact that the van der Waals attractive interactions between ions of ILs and water molecules increase as the molecular size of ILs increase. However, the osmotic coefficient of [C_4mim][MSO_4] solution is higher than that of [C_3mim][MSO_4] solution at the same molality and same temperature, as shown in Figure 6. Furthermore, concerning

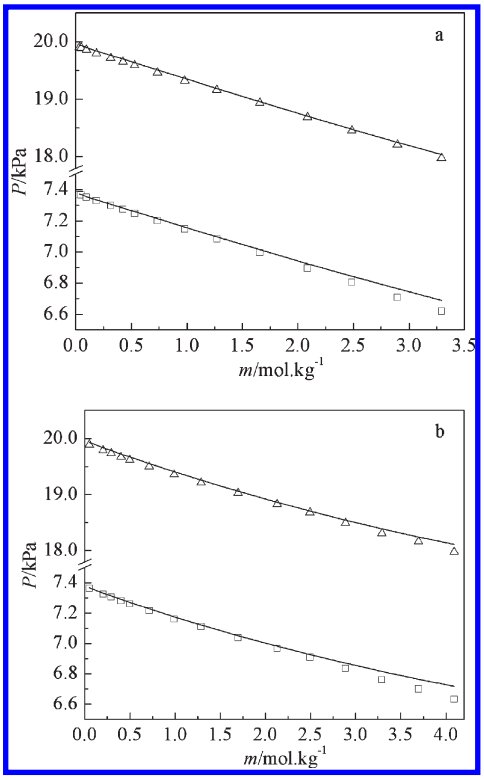

Figure 7. Vapor−liquid equilibria of aqueous IL solutions of (a) [C_1mim][MSO_4] and (b) [C_4mim][MSO_4]. Comparison between the predictions of the new model (lines) and the experimental data[31] (symbols): (□) 313; (Δ) 333 K).

the aqueous solutions of ILs containing the same cation, like [C_4mim][Br], [C_4mim][BF_4], and [C_4mim][MSO_4], the osmotic coefficient does not exhibit a clear trend as the size of the anions or surface charge density are changed (see Figure 6). Generally, for the studied systems, the experimental osmotic coefficients are well described by the new model.

4.3. Vapor−Liquid Equilibria. The vapor pressure of the studied ILs aqueous solutions have been predicted by using the ionic and association parameters listed in Tables 2 and 3. To perform these calculations we have assumed that the ILs cannot be vaporized. Thus, the vapor−liquid equilibrium equation for mixtures containing ILs at a fixed temperature can be written as

$$\varphi_w^V = x_w^L \varphi_w^L \quad (63)$$

where x_w^L and φ_w^L are the mole fraction and fugacity coefficient of water in liquid phase, respectively, and φ_w^V the fugacity coefficient of pure water in the vapor phase at the same temperature T and pressure P. A comparison of the VLE for [C_1mim][MSO_4] (a) and [C_4mim][MSO_4] (b) aqueous solution at temperature of 313 and 333 K and molality up to 4 mol·kg^{-1} are illustrated in Figure 7. As can be seen, the theoretical and experimental data[31] are in very good agreement. Since the vapor pressures are directly related to the activity of water, this result is expected as the new model accurately describes the osmotic coefficients (see section 4.2). However, one should mention that large deviations for the vapor pressures can be observed for highly concentrated IL aqueous solutions. As shown in Figure 8, the deviations become significant when the molality is largely above the maximum molality used in the parameter optimization. In this figure, the

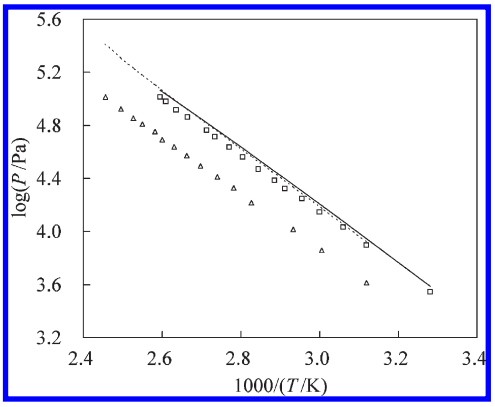

Figure 8. Vapor−liquid equilibria of aqueous solutions of [C_4mim][Br] at different IL concentrations. Comparison the predictions of the new model (line) and the experimental data[83] (symbol): Mole fraction of (□) 0.2; (Δ) 0.4; (solid line) 0.2; (dash line) 0.4).

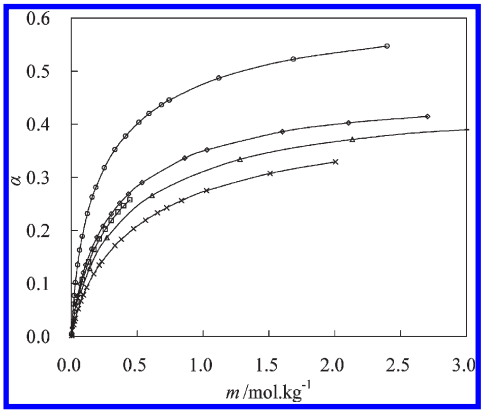

Figure 9. Degree of ionic association as a function of molality predicted at 308 K, in aqueous solutions of [$C_x$mim][Br]: (□) C_2; (◇) C_3; (Δ) C_4; (×) C_5; (○) C_6.

symbols of square and triangle denote the experimental vapor pressures of aqueous [C_4mim][Br] solutions[83] at the IL mole fraction 0.2 (about 13.88 mol·kg^{-1}) and 0.4 (about 37.0 mol·kg^{-1}), respectively, while the maximum molality used in the parameter adjustment for [C_4mim][Br] solution was only 7.79 mol/kg (Table 4). The model can well reproduce the experimental data at the mole fraction 0.2 (solid line in Figure 8), while the predictions are not accurate at the mole fraction 0.4 (dash line in Figure 8). Therefore, the model parameters summarized in Tables 2 and 3 should be applied with great care for predicting the thermodynamic properties of the IL aqueous solutions outside the concentration range of the experimental data.

4.4. Ionic Association. A detailed description of the ionic association between cations and anions of an IL in aqueous solution can also be provided by the new model. Our approach requires less parameters than other models to treat ionic association in weak electrolyte aqueous solutions.[59] The degree of ionic association degree between cations and anions has been determined for aqueous solutions of [$C_x$mim][Br] ($x = 2, ..., 6$) at 308.15 K, and is depicted in Figure 9. It can say that the degree of association at a given molality generally increases with the increasing alkyl chain length of the cations although this trend

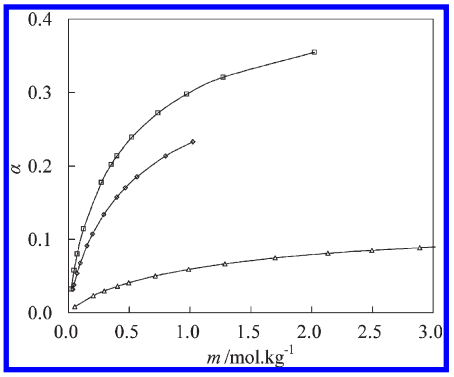

Figure 10. Degree of ionic association as a function of molality predicted at 318 K, in aqueous solutions of $[C_4mim][An]$: An = (□) Br; (◇) BF_4; (Δ) MSO_4.

is not very clear due to the complex influence of ionic segment diameter and associating energy on association degree, which increases with the increasing ionic association energy and segment diameter while the obtained model parameters of both for this series $[C_xmim][Br]$ have an opposite trend with respect to their corresponding molecular weight. Anyway, this trend is very similar to that observed experimentally.[25] This can be explained by hydrophobic interactions. In such aqueous solution of ILs, the hydration of the cations is weakened with the increasing alkyl chain length, leading to an enhancement of ion pairing. One can also compare the ionic associations of the ILs $[C_4mim][An]$ (An = Br, BF_4, and MSO_4) in aqueous solution. As can be seen in Figure 10, the degree and energy of association decreases as follows $[Br]^- > [BF_4]^- > [MSO_4]^-$. One can observe that the association ability of anions decreases with the decrease of their surface charge density. However, the predicted trend is different from that observed experimentally:[25] for the $[C_4mim][An]$ ILS, the association degree is higher for $[BF_4]^-$ than for $[Br]^-$. This may be explained by a higher solvation of the $[Br]^-$ anion due to a higher surface charge density.[25] Note that it was experimentally observed that the ionic association ability of the $[BF_4]^-$ anion is stronger than that of $[PF_6]^-$.[25]

One can also predict the equilibrium constant K_a of ion association from the new model by using an extrapolation up to the infinite dilution limit. The equilibrium constant K_a for ionic association is defined with respect to the following chemical equilibrium, $[Cat]^+ + [An]^- \leftrightarrow [Cat][An]$. At infinite dilution in pure water (reference state), the activity coefficients of all species equal to 1, and K_a can be written as

$$K_a = \frac{\alpha}{C_0(1-\alpha)^2} \quad (64)$$

where C_0 is the initial concentration of the IL solute molecule and α the degree of ionic association. According to eq 64, the K_a value at infinite dilution can be estimated at the limit $C_0 \rightarrow 0$ by extrapolation: here we assume that the infinite solute concentration is equal to 10^{-3} mol·L^{-1}. We have estimated K_a at 298.15 K for $[C_6mim][Br]$ and have obtained K_a = 4.94 L.mol^{-1}, which is in excellent agreement with the literature value (4.9 L·mol^{-1}) provided by Shekaari et al.,[84] however, less than the value 71 ± 8 L·mol^{-1} reported by Wang et al.[25] As shown by Wang et al.,[25] the large discrepancy for the values of the ionic association constant for $[C_6mim][Br]$ among the different experimental studies may result from that fact that K_a was determined over different concentration ranges more or less far from the infinite dilution limit. It is indeed clear that the activity coefficients of the ions and the osmotic coefficients decrease dramatically from 1 as the concentration of the solute is increased in the dilute range. Thus, eq 64 is only valid for very dilute solutions. Another reason for the differences between the calculated K_a and the experimental values may be the fact that the experimental K_a values were determined from the measurements of conductivity and the Lee−Wheaton equation,[85] as suggested by Pethybridge and Taba,[86] while our predictions of K_a are obtained from an EOS fitted to experimental liquid densities and osmotic coefficients. The differences can also be explained by the experimental uncertainties and the realism of the model.

5. CONCLUSIONS

The SWCF-VR EOS has been extended to describe thermodynamic properties of aqueous ionic liquid solutions. The new model takes both electrostatic charge−charge interactions and ionic associations into account and is able to accurately describe the liquid densities, osmotic coefficients, and vapor pressures of IL solutions. Moreover, we are able to determine the equilibrium constant of the association between cations and anions of ILs in water. The predicted ionic association constants are generally consistent with experimental data. The model parameters (the segment diameter, dispersion energy, and well width) are used to characterize each ion, and the ions and their parameters are transferable from one IL to another. In contrast to other thermodynamic models for common electrolyte solutions, the new model can not only reproduce the experimental thermodynamic properties of ILs but also provide useful information on the ionic association equilibrium. Therefore, this model can be used for both strong and weak electrolyte solutions, and no additional parameter accounting for the association/dissociation equilibrium is needed. However, the new model cannot simultaneously calculate the properties of pure ILs and aqueous IL solutions using the same molecular parameters as given in the present work yet; only the thermodynamic properties of aqueous solutions are modeled. The extension to pure ILs and common strong and weak electrolyte solutions as well as protein solutions is the goal of future work.

AUTHOR INFORMATION

Corresponding Author

*Tel./Fax: 86-21-6425 2767. E-mail: cjpeng@ecust.edu.cn.

ACKNOWLEDGMENT

The authors from the East China University of Science and Technology appreciate the financial support by the National Natural Science Foundation of China (Nos. 20776040, 20876041 and 20736002), the National Basic Research Program of China (2009CB219902), the program for Changjiang Scholars and the Innovative Research Team in University of China (Grant IRT0721), and the 111 Project (Grant B08021) of China. J.L. and P.P. thank the financial support of the French Research National Agency (ANR-09-CP2D-10-03).

NOMENCLATURE

A = Helmholtz free energy
a_2, b_2, c_2, a_3, b_3, c_3 = model constant

a_w = activity
g = radial distribution function
I_1,I_2 = abbreviations, defined by eqs 11 and 12
K^{hs} = isothermal compressibility
K = number of component
K_a = chemical equilibrium constant in $L \cdot mol^{-1}$
k = Boltzmann constant
m = molality in $mol \cdot kg^{-1}$
P = pressure
r = segment number
T = temperature in K
V = volume
x = Mole fraction
y = cavity correlation function
z = charge number

Greek Letters

α = degree of association between cations and anions
α_2, β_2, γ_2, α_3, β_3, γ_3 = model constants
γ_w = activity coefficient
ζ = parameters defined in eq 5
ξ_1, ξ_2, ξ_3 = model parameters, defined by eq 13
ξ_a, ξ_b, ξ_c = model parameters, defined by eq 29
ε/k = dispersion energy in K
η = reduced segment density
k_{ij} = adjusted binary parameter
λ = reduced well width of the square-well potential
ρ_0 = molecular number density
ρ_s = segment number density
σ = segment collision diameter in Å
ϕ = segment fraction or osmotic coefficient

Subscripts

an = anion
cat = cation
i,j = Pure component indexes
ij,ji = interaction of component i and j
S_iS_{i+1} = nearest-neighbor pairs
S_iS_{i+2} = next-to-nearest-neighbor pairs

REFERENCES

(1) Cole-Hamilton, D. J. Homogeneous catalysis-new approaches to catalyst separation, recovery and recycling. *Science* **2003**, *299*, 1702–1706.

(2) Zhou, F.; Liang, Y.; Liu, W. Ionic liquid lubricants: designed chemistry for engineering applications. *Chem. Soc. Rev.* **2009**, *38*, 2590–2599.

(3) Wasserscheid, P.; Welton, T. *Ionic Liquids in Synthesis*; Wiley-Verlag: Weinheim, Germany, 2003.

(4) Plechkova, N. V.; Seddon, K. R. Application of ionic liquids in the chemical industry. *Chem. Soc. Rev.* **2008**, *37*, 123–150.

(5) Heintz, A. Recent developments in thermodynamics and thermophysics of non-aqueous mixtures contaning ionic liquids. A review. *J. Chem. Thermodyn.* **2005**, *37*, 525–535.

(6) Zhang, S.; Lu, X.; Zhou, Q.; Li, X.; Zhang, X.; Li, S. *Ionic liquids: Physicochemical Properties*; Elsevier: Amsterdam, 2009.

(7) Aparicio, S.; Atilhan, M.; Karadas, F. Thermophysical properties of pure ionic liquids: Review of present situation. *Ind. Eng. Chem. Res.* **2010**, *49*, 9580–9595.

(8) Vega, L. F.; Vilaseca, O.; Llovell, F.; Andreu, J. S. Modeling ionic liquids and the solubility of gases in them: Recent advances and perspectives. *Fluid Phase Equilib.* **2010**, *294*, 15–30.

(9) Belzeve, L. S.; Brennecke, J. F.; Stadtherr, M. A. Modeling of activity coefficients of aqueous solutions of quaternary ammonium salts with the electrolyte−NRTL equation. *Ind. Eng. Chem. Res.* **2004**, *43*, 815–825.

(10) Huo, Y.; Xia, S.; Yi, S.; Ma, P. Measurement and correlation of vapor pressure of benzene and thiophene with [Bmim][PF_6] and [Bmim][BF_4] ionic liquids. *Fluid Phase Equilib.* **2009**, *276*, 46–52.

(11) Simoni, L. D.; Lin, Y.; Brennecke, J. F.; Stadtherr, M. A. Modeling liquid−liquid equilibrium of ionic liquid systems with NRTL, electrolyte-NRTL, and UNIQUAC. *Ind. Eng. Chem. Res.* **2008**, *47*, 256–272.

(12) Simoni, L. D.; Chapeaux, A.; Brennecke, J. F.; Stadtherr, M. A. Asymmetric Framework for predicting liquid−liquid equilibrium of ionic liquid mixed solvent systems. 2. Prediction of Ternary system. *Ind. Eng. Chem. Res.* **2009**, *48*, 7257–7265.

(13) Scovazzo, P.; Camper, D.; Kieft, J.; Poshusta, J.; Koval, C.; Noble, R. Regular solution theory and CO_2 gas solubility in room temperature ionic liquids. *Ind. Eng. Chem. Res.* **2004**, *43*, 6855–6860.

(14) Wang, J.; Sun, W.; Li, C.; Wang, Z. Correlation of infinite dilution activity coefficient of solute in ionic liquid using UNIFAC model. *Fluid Phase Equilib.* **2008**, *264*, 235–241.

(15) Carvalho, P. J.; Alvarez, V. H.; Machado, J. J. B.; Pauly, J.; Daridon, J. L.; Marrucho, I. M.; Aznar, M.; COutinho, J. A. P. High pressure phase behavior of carbon dioxide in 1-alkyl-3-methylimidazolium bis(trifluoromethylsulfonyl)imide ionic liquids. *J. Supercrit. Fluids* **2009**, *48*, 99–107.

(16) Kroon, M. C.; Karakatsani, E. K.; Economou, I. G.; Witkamp, G. J.; Peters, C. J. Modeling of the carbon dioxide solubility in imidazolium-based ionic liquids with the tPC-SAFT equation of state. *J. Phys. Chem. B* **2006**, *110*, 9262–9269.

(17) Karakatsani, E. K.; Economou, I. G.; Kroon, M. C.; Peters, C. J.; Witkamp, G. J. tPC-PSAFT modeling of gas solubility in imidazolium-based ionic liquids. *J. Phys. Chem. C* **2007**, *111*, 15487–15492.

(18) Andreu, J. S.; Vega, L. F. Capturing the solubility behavior of CO_2 in ionic liquids by a simple model. *J. Phys. Chem. C* **2007**, *111*, 16028–16034.

(19) Wang, T. F.; Peng, C. J.; Liu, H. L.; Hu, Y. Description of the *pVT* behavior of ionic liquids and the solubility of gases in ionic liquids using an equation of state. *Fluid Phase Equilib.* **2006**, *205*, 150–157.

(20) Li, J. L.; He, Q.; He, C. C.; Peng, C. J.; Liu, H. L. Representation of phase behavior of ionic liquids using the equation of state for square well chain fluids with variable range. *Chin. J. Chem. Eng.* **2009**, *17*, 983–989.

(21) Wang, T. F.; Peng, C. J.; Liu, H. L.; Hu, Y.; Jiang, J. W. An equation of state for the vapor−liquid equilibria of binary systems containing imidazolium-based ionic liquid. *Ind. Eng. Chem. Res.* **2007**, *46*, 4323–4329.

(22) Ji, X.; Adidharma, H. Thermodynamic modeling of ionic liquid density with heterosegmented statistical associating fluid theory. *Chem. Eng. Sci.* **2009**, *64*, 1985–1992.

(23) Dorbritz, S.; Ruth, W.; Kragl, U. Investigation on aggregate formation of ionic liquids. *Adv. Synth. Catal.* **2005**, *347*, 1273–1279.

(24) Wang, Y.; Voth, G. A. Unique spatial heterogeneity in ionic liquids. *J. Am. Chem. Soc.* **2005**, *127*, 12192–12193.

(25) Wang, H.; Wang, J.; Zhang, S.; Pei, Y.; Zhuo, K. Ionic association of the ionic liquids [C_4mim][BF_4], [C_4mim][PF_6], and [$C_n$mim][Br] in molecular solvents. *Chem. Phys. Chem.* **2009**, *10*, 2516–2523.

(26) Gardas, R. L.; Dagade, D. H.; Coutinho, J. A. P.; Patil, K. J. Thermodynamic studies of ionic interactions in aqueous solutions of imidazolium based ionic liquids [Emim][Br] and [Bmim][Cl]. *J. Phys. Chem. B* **2008**, *112*, 3380–3389.

(27) Shekaari, H.; Mousavi, S. S. Influence of alkyl chain on the thermodynamic properties of aqueous solutions of ionic liquids 1-alkyl-3-methylimidazolium bromide at different temperatures. *J. Chem. Thermodyn.* **2009**, *41*, 90–96.

(28) Sadeghi, R.; Shekaari, H.; Hosseini, R. Effect of alkyl chain length and temperature on the thermodynamic properties of ionic liquids 1-alkyl-3-methylimidazolium bromide in aqueous and non-aqueous solutions at different temperatures. *J. Chem. Thermodyn.* **2009**, *41*, 273–289.

(29) Shekaari, H.; Zafarani-Moattar, M. T. Osmotic coefficients of some imidazolium based ionic liquids in water and acetonitrile at temperature 318.15 K. *Fluid Phase Equilib.* **2007**, *254*, 198–203.
(30) Zafarani-Moattar, M. T.; Shekaari, H. Apparent molar volume and isentropic compressibility of ionic liquid 1-butyl-3-methylimidazolium bromide in water, methanol, and ethanol at T = (298.15 to 318.15) K. *J. Chem. Thermodyn.* **2005**, *37*, 1029–1035.
(31) Gonzalez, B.; Calvar, N.; Dominguez, A.; Macedo, E. A. Osmotic coefficients of aqueous solutions of four ionic liquids at T = (313.15 and 333.15) K. *J. Chem. Thermodyn.* **2008**, *40*, 1346–1351.
(32) Shekaari, H.; Armanfar, E. Physical properties of aqueous solutions of ionic liquid, 1-propyl-3-methylimidazolium methyl sulfate, at T = (298.15 to 328.15) K. *J. Chem. Eng. Data* **2010**, *55*, 765–772.
(33) Blum, L. Mean spherical model for asymmetric electrolytes 1. Method of solution. *Mol. Phys.* **1975**, *30*, 1529–1535.
(34) Blum, L.; Hoeye, J. S. Mean spherical model for asymmetric electrolytes. 2. Thermodynamic properties and the pair correlation function. *J. Phys. Chem.* **1977**, *81*, 1311–1316.
(35) Percus, J. K.; Yevick, G. Hard-core insertion in the many-body problem. *Phys. Rev.* **1964**, *136*, B290–B296.
(36) Lebowitz, J. L.; Percus, J. K. Mean spherical model for lattice gases with extended hard cores and continuum fluids. *Phys. Rev.* **1966**, *144*, 251–258.
(37) Waisman, E.; Lebowitz, J. L. Mean spherical model integral equation for charged hard spheres I. Method of solution. *J. Chem. Phys.* **1972**, *56*, 3086–3093.
(38) Waisman, E.; Lebowitz, J. L. Mean spherical model integral equation for charged hard spheres II. Results. *J. Chem. Phys.* **1972**, *56*, 3093–3099.
(39) Liu, W. B.; Li, Y. G.; Lu, J. F. A new equation of state for real aqueous ionic fluids based on electrolyte perturbation theory, mean spherical approximation and statistical associating fluid theory. *Fluid Phase Equilib.* **1999**, *158*−*160*, 595–606.
(40) Huang, S. H.; Radosz, M. Equation of state for small, large, polydisperse, and associating molecules. *Ind. Eng. Chem. Res.* **1990**, *29*, 2284–2294.
(41) Huang, S. H.; Radosz, M. Equation of state for small, large, polydisperse, and associating molecules: Extension to fluid mixtures. *Ind. Eng. Chem. Res.* **1991**, *30*, 1994–2005.
(42) Galindo, A.; Gil-Villegas, A.; Jackson, G.; Burgess, A. N. SAFT-VRE: Phase behavior of electrolyte solutions with the statistical associating fluid theory for potentials of variable range. *J. Phys. Chem. B* **1999**, *103*, 10272–10281.
(43) Gil-Villegas, A.; Galindo, A.; Jackson, G. A statistical associating fluid theory for electrolyte solutions (SAFT-VRE). *Mol. Phys.* **2001**, *99*, 531.
(44) Patel, B. H.; Paricaud, P.; Galindo, A.; Maitland, G. C. Prediction of the salting-out effect of strong electrolytes on water + alkane solutions. *Ind. Eng. Chem. Res.* **2003**, *42*, 3809–3823.
(45) Tan, S. P.; Adidharma, H.; Radosz, M. Statistical associating fluid theory coupled with restricted primitive model to represent aqueous strong electrolytes. *Ind. Eng. Chem. Res.* **2005**, *44*, 4442–4452.
(46) Ji, X. Y.; Tan, S. P.; Adidharma, H.; Radosz, M. Statistical associating fluid theory coupled with restricted primitive model to represent aqueous strong electrolytes multiple salt solutions. *Ind. Eng. Chem. Res.* **2005**, *44*, 7584–7590.
(47) Tan, S. P.; Ji, X. Y.; Adidharma, H.; Radosz, M. Statistical associating fluid theory coupled with restrictive primitive model extended to bivalent ions. SAFT2: 1. Single salt + water solutions. *J. Phys. Chem. B* **2006**, *110*, 16694–16699.
(48) Ji, X. Y.; Adidharma, H. Ion-based SAFT2 to represent aqueous single- and multiple-salt solutions at 298.15 K. *Ind. Eng. Chem. Res.* **2006**, *45*, 7719–7728.
(49) Ji, X. Y.; Adidharma, H. Ion-based statistical associating fluid theory (SAFT2) to represent aqueous single-salt solutions at temperatures and pressures up to 473.15 K and 1000 bar. *Ind. Eng. Chem. Res.* **2007**, *46*, 4667–4677.
(50) Adidharma, H.; Radosz, M. A prototype of an engineering equation of state for hetero-segmented polymers. *Ind. Eng. Chem. Res.* **1998**, *37*, 4453–4462.
(51) Liu, Y.; Li, Z. B.; Mi, J. G.; Zhong, C. L. Modeling of aqueous electrolyte solutions based on primitive and first-order mean spherical approximation. *Ind. Eng. Chem. Res.* **2008**, *47*, 1695–1701.
(52) Liu, Z. P.; Wang, W. C.; Li, Y. G. An equation of state for electrolyte solutions by a combination of low-density expansion of nonprimitive mean spherical approximation and statistical associating fluid theory. *Fluid Phase Equilib.* **2005**, *227*, 147–156.
(53) Gil-Villegas, A.; Galindo, A.; Whitehead, P. J.; Mills, S. J.; Jackson, G.; Burgess, A. N. Statistical associating fluid theory for chain molecules with attractive potentials of variable range. *J. Chem. Phys.* **1997**, *106*, 4168–4175.
(54) Gross, J.; Sadowski, G. Application of perturbation theory to a hard-chain reference fluid: An equation of state for square-well chains. *Fluid Phase Equilib.* **2000**, *168*, 183–199.
(55) Zhao, H.; dos Ramos, M. C.; McCabe, C. Development of an equation of state for electrolyte solutions by combining the statistical associating fluid theory and the mean spherical approximation for the nonprimitive model. *J. Chem. Phys.* **2007**, *126*, 244503-1–244503-14.
(56) Herzog, S.; Gross, J.; Arlt, W. Equation of state for aqueous electrolyte systems based on the semirestricted nonprimitive mean spherical approximation. *Fluid Phase Equilib.* **2010**, *297*, 23–33.
(57) Cameretti, L. F.; Sadowski, G.; Mollerup, J. M. Modeling of aqueous electrolyte solutions with perturber-chain statistical associated fluid theory. *Ind. Eng. Chem. Res.* **2005**, *44*, 3355–3362.
(58) Held, C.; Cameretti, L. F.; Sadowski, G. Modeling aqueous electrolyte solutions Part I. Fully dissociated electrolytes. *Fluid Phase Equilib.* **2008**, *270*, 87–96.
(59) Held, C.; Sadowski, G. Modeling aqueous electrolyte solutions. Part 2. Weak electrolytes. *Fluid Phase Equilib.* **2009**, *279*, 141–148.
(60) Paricaud, P.; Galindo, A.; Jackson, G. Recent advances in the use of the SAFT approach in describing electrolytes, interfaces, liquid crystals and polymers. *Fluid Phase Equilib.* **2002**, *194*−*197*, 87–96.
(61) Tan, S. P.; Adidharma, H.; Radosz, M. Recent advances and applications of statistical associating fluid theory. *Ind. Eng. Chem. Res.* **2008**, *47*, 8063–8082.
(62) Wang, J. F.; Li, C. X.; Shen, C.; Wang, Z. H. Towards understanding the effect of electrostatic interactions on the density of ionic liquids. *Fluid Phase Equilib.* **2009**, *279*, 87–91.
(63) Barker, J. A.; Henderson, D. Perturbation theory and equation of state for fluids: The square well potential. *J. Chem. Phys.* **1967**, *47*, 2856–2561.
(64) Chiew, Y. C. Percus-Yevick Integral-Equation Theory for Athermal Hard-Sphere Chains. II. Average Intermolecular Correlation Functions. *Mol. Phys.* **1991**, *73*, 359–373.
(65) Li, J. L.; He, H. H.; Peng, C. J.; Liu, H. L.; Hu, Y. A new development of equation of state for square-well chain-like molecules with variable width $1.1 \leq \lambda \leq 3$. *Fluid Phase Equilib.* **2009**, *276*, 57–68.
(66) Li, J. L.; He, H. H.; Peng, C. J.; Liu, H. L.; Hu, Y. Equation of state for square-well chain molecules with variable range. I: Application for pure substances. *Fluid Phase Equilib.* **2009**, *286*, 8–16.
(67) Li, J. L.; Tong, M.; Peng, C. J.; Liu, H. L.; Hu, Y. Equation of state for square-well chain molecules with variable range. II: Extension to mixture. *Fluid Phase Equilib.* **2009**, *287*, 56–67.
(68) He, C. C.; Li, J. L.; Ma, J.; Peng, C. J.; Liu, H. L.; Hu, Y. Eqution of state for square well chain molecules with variable range. Extension to associating fluids. *Fluid Phase Equilib.* **2011**, *302*, 139–152.
(69) Liu, H. L.; Hu, Y. Equation of state for systems containing chainlike molecules. *Ind. Eng. Chem. Res.* **1998**, *37*, 3058–3066.
(70) Cummings, P. T.; Stell, G. Statistical mechanical models of chemical reactions. Analytic solution of models of A+B reversible AB in the Percus−Yevick approximation. *Mol. Phys.* **1984**, *51*, 253–287.
(71) Cummings, P. T.; Stell, G. Statistical mechanical models of chemical reactions 2. Analytic solution of the Percus−Yevick approximation for a model of homogeneous association. *Mol. Phys.* **1985**, *55*, 33–48.
(72) Mansoori, G. A.; Carnahan, N. F.; Starling, K. E.; Leland, T. W. Equilibrium thermodynamic properties of the mixture of hard spheres. *J. Chem. Phys.* **1971**, *54*, 1523–1525.

(73) Rowlinson, J. S.; Swinton, F. L. *Liquids and liquid mixtures*, 3rd ed.; Butterworth: London, 1982.
(74) Hu, Y.; Liu, H. L.; Prausnitz, J. M. Equation of state for fluids containing chainlike molecules. *J. Chem. Phys.* **1996**, *104*, 396–404.
(75) Wertheim, M. S. Fluids with highly directional attractive forces. I. Statistical thermodynamics. *J. Stat. Phys.* **1984**, *35*, 19–34.
(76) Wertheim, M. S. Fluids with highly directional attractive forces. II. Thermodynamic perturbation theory and integral equations. *J. Stat. Phys.* **1984**, *35*, 35–47.
(77) Wertheim, M. S. Fluids with highly directional attractive forces. III. Multiple attraction sites. *J. Stat. Phys.* **1986**, *42*, 459–476.
(78) Wertheim, M. S. Fluids with highly directional attractive forces. IV. Equilibrium polymerization. *J. Stat. Phys.* **1986**, *42*, 477–492.
(79) Blum, L. *Theoretical Chemistry: Advances and Perspectives*; Henderson, D., Ed.; Academic: New York, 1980; Vol. 5.
(80) Kiepe, J.; Noll, O.; Gmehling, J. Modified LIQUAC and modified LIFAC—A further development of electrolyte models for the reliable prediction of phase equilibria with strong electrolytes. *Ind. Eng. Chem. Res.* **2006**, *45*, 2361–2373.
(81) Held, C.; Cameretti, L. F.; Sadowski, G. Modeling aqueous electrolyte solutions Part 1. Fully dissociated electrolytes. *Fluid Phase Equilib.* **2008**, *270*, 87–96.
(82) Bini, R.; Bortolini, O.; Chiappe, C.; Pieraccini, D.; Siciliano, T. Development of cation/anion "interaction" scales for ionic liquids through ESI-MS measurements. *J. Phys. Chem. B* **2007**, *111*, 598–604.
(83) Kim, K. S.; Park, S. Y.; Choi, S.; Lee, H. Vapor pressures of the 1-butyl-3-methylimidazolium bromide + water, 1-butyl-3-methylimidazolium tetrafluoroborate + water, and 1-(2-hydroxyethyl)-3-methylimidazolium tetrafluoroborate + water systems. *J. Chem. Eng. Data* **2004**, *49*, 1550–1553.
(84) Shekaari, H.; Mansoori, Y.; Sadeghi, R. Density, speed of sound, and electrical conductance of ionic liquid 1-hexyl-3-methyl-imidazolium bromide in water at different temperataures. *J. Chem. Thermodyn.* **2008**, *40*, 852–859.
(85) Lee, W. H.; Wheaton, R. J. Conductance of symmetrical, unsymmetrical and mixed electrolytes. 3. Examination of new model and analysis of data for symmetrical electrolytes. *J. Chem. Soc., Faraday Trans. II* **1979**, *75*, 1128–1145.
(86) Pethybridge, A. D.; Taba, S. S. Precise conductimetric studies on aqueous-solutions of 2−2 electrolytes. 2. Analysis of data for $MgSO_4$ in terms of new equations from Fuoss and from Lee and Wheaton. *J. Chem. Soc., Faraday I* **1980**, *76*, 368–376.